Mineralogical model of lower mantle inferred from high-pressure and -temperature sound velocity data

It is widely accepted that at least the Earth's uppermost mantle, perhaps down to the top of the mantle transition zone, has a peridotitic (pyrolitic) bulk composition, on the basis of petrological evidence. On the other hand, a variety of chemical compositions, ranging from peridotitic to chondritic, have been proposed for the lower mantle. This has long remained controversial owing to the lack of conclusive arguments. The mineral assemblage of the lower mantle has been examined from density measurements under high *P-T* conditions. However, recent computational simulations demonstrated that such experimentally derived density and bulk moduli do not place unique constraints on the mantle composition because of their intrinsic uncertainties, whereas shear velocity (V_S) data strongly constrain the lower mantle models. It is thus crucial to obtain reliable V_S data of the major lower mantle constituents, silicate perovskite (pv) and (Mg,Fe)O ferropriclase (fp), under relevant high *P-T* conditions. Recent progress in Brillouin scattering spectroscopy optimized for extreme high-pressure conditions has so far enabled us to measure V_S of $MgSiO_3$-pv [1], post-perovskite [2], and MgO periclase [3] up to 172 GPa. Although those sound velocity data indeed provide valuable information on the lower mantle mineralogy, the effects of chemical impurities, such as iron and aluminum, and high temperature remain unsettled. More importantly, sound velocity measurements of pv and fp have never been performed under simultaneously high-*P* and high-*T* conditions corresponding to the lower mantle environment. Here, we determined V_S of aluminous silicate pv and fp up to 124 GPa at 300 K. The high *P-T* measurements were also conducted on $MgSiO_3$ pv and MgO at a temperature of 2700 K up to 91 GPa using the newly developed Brillouin scattering system at beamline **BL10XU** [4,5].

We obtained very sharp Brillouin peaks from the transverse acoustic modes of each phase over the entire *P-T* range we explored (Fig. 1). No significant peak broadening was observed with increasing pressure. The angle-dispersive synchrotron X-ray diffraction measurements were conducted simultaneously to determine the volume of the sample and the pressure at BL10XU, the synchrotron X-ray source of SPring-8 in the energy range of 30–50 keV. The X-ray diffraction peaks for each sample were very sharp, and two-dimensional X-ray diffraction images showed clear circular Debye rings with fairly uniform intensity distribution along the circle, indicating that the sample did not undergo significant grain growth or lattice preferred orientation under high pressure and high temperature. On the basis of the fit of the finite strain to the *P*-V_S profiles of Al-pv and fp, we obtained the best-fit values of G_0 = 166(1) GPa (shear modulus) and G_0' = 1.57(5) (pressure derivative of shear modulus) for Al-pv. The G_0' of Al-pv coincides with the 1.56(4) of pure $MgSiO_3$ pv, indicating a minimal effect of Al on G_0'. For fp, the finite strain was fitted separately for low- (5–40 GPa) and high- (60–121 GPa) pressure ranges, because anomalous behavior was observed around 50 GPa owing to spin crossover. The fitting result gives G_0 = 113(2) GPa and G_0' = 2.15(5) for the HS state, and G_0 = 130(2) GPa and G_0' = 2.04(5) for the LS state. Extrapolation of the HS data to high pressure does not reproduce the LS data, supporting the claim that the spin crossover of iron is not associated with the elastic softening. These G_0 and G_0' values for Al-pv and fp are plotted together with previous data in Fig. 2 as a function of iron or aluminum content. With such relationships, we can estimate G_0 and G_0' for the representative mantle composition (X_{Mg} = 79 for fp and X_{Al2O3} = 4 wt% for pv). The high *P-T* measurements on pure $MgSiO_3$ pv and MgO showed the velocity reduction by ~4% and ~6%, respectively, on average at 2700 K from the room-*T* data at lower mantle pressures. A linear fitting of the shear moduli against pressure, combined with the reported values of G_0 and G_0' [1,3], provides temperature derivatives of the shear modulus: dG/dT = –0.020(1) GPa/K for both pv and MgO. The shear strain derivatives of the

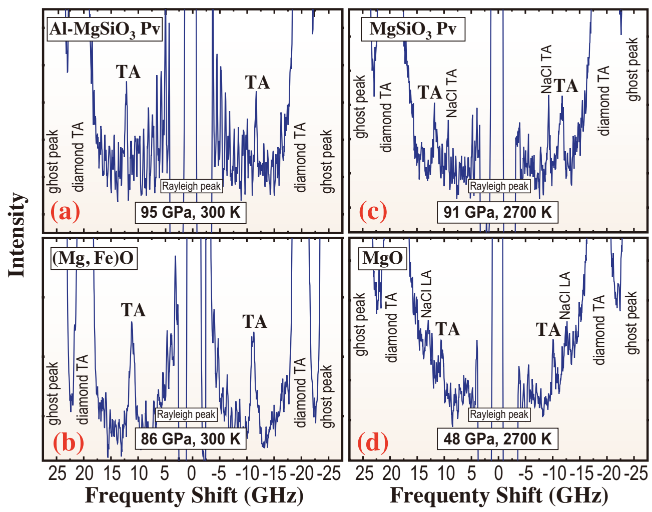

Fig. 1. Brillouin spectra of lower mantle phases: **(a)** $MgSiO_3$(+4 wt% Al_2O_3) pv at 95 GPa/300 K; **(b)** $(Mg_{0.92}Fe_{0.08})O$ at 86 GPa/300 K; **(c)** $MgSiO_3$ pv at 91 GPa/2700 K; and **(d)** MgO at 48 GPa/2700 K. TA and LA indicate transverse and longitudinal acoustic modes of Brillouin shift, respectively.

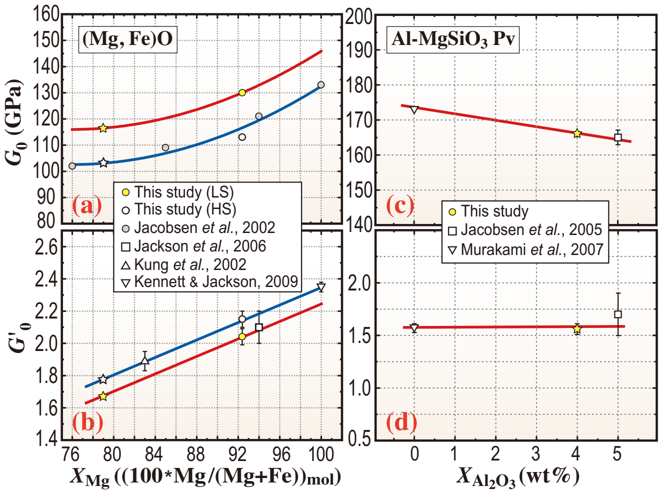

Fig. 2. Effect of Al and Fe on shear modulus (G_0) and its pressure derivative (G_0'). **(a,b)** (Mg,Fe)O fp, and **(c,d)** Al-bearing $MgSiO_3$ pv. Stars correspond to G_0 or G_0' for representative iron/alumina content of X_{Mg} = 79 mol% for fp and $X_{Al_2O_3}$ = 4 wt%. Lines show the best-fit trends. Blue and red lines in (a) and (b) indicate the trends of (Mg,Fe)O at HS and LS states of iron, respectively.

Grüneisen parameter (γ) are estimated to be η_{S0} = 2.4(2) for pv and 3.0(3) for MgO.

Present measurements performed over a wide *P-T* range that covers almost the entire range of lower mantle conditions allow us to constrain the lower mantle mineralogy. We model the lower mantle as a two-phase mixture of pv and fp in the SiO_2-MgO-FeO-Al_2O_3 system, in which (Al,Fe)-bearing pv contains 4 wt% Al_2O_3 with X_{Mg} = 94 and fp has X_{Mg} = 79. A constant Mg-Fe partitioning coefficient between pv and fp is assumed for the entire lower mantle. The V_S profiles of these pv and fp were calculated along the typical temperature profiles (Fig. 3(a)). The PREM is best fitted by the mixture of 95% pv and 5% fp in volume (X_{Pv} = 0.95) (Fig. 3(b)). The velocity of fp increases steeply by ~4% across the spin crossover, however, such an anomalous feature is not clear in the calculated profile of the pv+fp mixture, suggesting that the spin crossover of iron in fp may be seismologically invisible. On the other hand, the V_S profile for a peridotitic (pyrolitic) mantle (X_{Pv} = 0.80) is shown to be lower by up to 3.2% than the PREM throughout the pressure range of the lower mantle, indicating that the conventional peridotitic model is incompatible with the seismological observations.

The present results indicate that the conventional peridotitic mantle model is not compatible with the seismic properties of the lower mantle and suggest that the lower mantle is dominated by perovskite (~95 vol%) and therefore is silica-rich in comparison with the upper mantle. The different chemical compositions between the upper and lower mantle could be a consequence of fractional crystallization of the magma ocean extending to the deep lower mantle in the early history of the Earth. The primordial chemical stratification may have been preserved through the subsequent solid-state convection until the present day. The layered mantle convection is presumed to have been predominant in early Earth, indicating limited mass transport between the upper and lower mantle. The seismic tomography images of subducting slabs or upwelling plumes penetrating the upper/lower mantle boundary may not represent whole-mantle convection but intermittent/transitional stages between layered and whole mantle-convections.

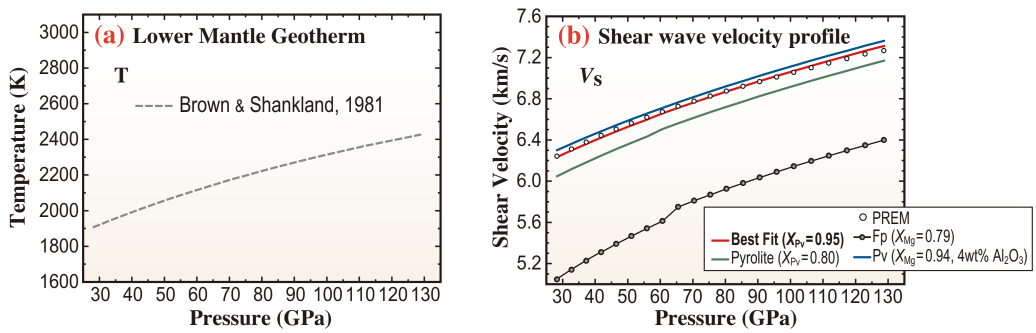

Fig. 3. Representative lower mantle geotherm **(a)** and calculated shear wave velocity profiles of fp (black lines) and pv (blue lines) **(b)**. Velocity profile for the pyrolite model is shown as the green line. Best-fit model to the PREM is shown as a red curve.

Motohiko Murakami

Department of Earth and Planetary Materials Sciences, Tohoku University

Email: motohiko@m.tohoku.ac.jp

References

[1] M. Murakami *et al.*: Earth Planet. Sci. Lett. **256** (2007) 47.
[2] M. Murakami *et al.*: Earth Planet. Sci. Lett. **259** (2007) 18.
[3] M. Murakami *et al.*: Earth Planet. Sci. Lett. **277** (2009) 123.
[4] M. Murakami *et al.*: Phys. Earth Planet. Inter. **174** (2009) 282.
[5] *M. Murakami, Y. Ohishi, N. Hirao and K. Hirose: Nature* ***485*** *(2012) 90.*